Downloaded from ascelibrary.org by University of Wisconsin-Madison on 05/24/23. Copyright ASCE. For personal use only; all rights reserved.

Unit Weight of Water in Clayey Soil

Shengmin Luo, A.M.ASCE[1]; Baochun Zhou[2]; Jing Peng, Ph.D., S.M.ASCE[3];
William J. Likos, M.ASCE[4]; and Ning Lu, F.ASCE[5]

Abstract: A soil water unit weight of 9.8 kN/m^3 has been universally considered to quantify soil volumetric phase properties such as void ratio and degree of saturation, but has been found to greatly vary depending on soil type and the volume scale with which it is defined. Recent experimental and theoretical evidence has indicated that the unit weight of soil water can be significantly greater than 9.8 kN/m^3 for clayey soils when gravimetric water content is less than 30%. A soil water unit weight as high as 18.8 kN/m^3 is evident for some expansive soils at low water content. The significance of abnormally high water unit weight in quantifying soil phase volumes, saturation, and void ratio was experimentally assessed for various clayey soils and theoretically interpreted as a function of water content and soil type. For clayey soils with low liquid limit, average soil water unit weight can be as high as 12.5 kN/m^3 for gravimetric water content less than 10%. This leads to an overestimation of liquid-phase saturation and void ratio by as much as 8% if a soil water unit weight of 9.8 kN/m^3 is used. For clayey soil with a high liquid limit, the average soil water unit weight can be as high as 18.8 kN/m^3 for water content less than 18%, leading to overestimation of liquid-phase saturation by as much as 36% and void ratio by as much as 20% if 9.8 kN/m^3 is used. Charts were developed to estimate average soil water unit weight as a function of soil specific surface area and water content, and as a function of liquid limit and water content. The commonly used value of 9.8 kN/m^3 for water unit weight can lead to significant errors in estimating phase volumes, void ratio, and saturation for clayey soils. **DOI: 10.1061/JGGEFK.GTENG-10844.** *© 2022 American Society of Civil Engineers.*

Author keywords: Soil water unit weight; Pore water pressure; Soil phase diagram; Specific surface area; Adsorbed water; Capillary water.

Introduction

The soil water unit weight (kN/m^3) is defined as the soil water mass per unit of soil water volume. Soil water unit weight has been widely considered in geotechnical and geoenvironmental engineering practice to be a constant value equal to the unit weight of free water, or 9.8 kN/m^3. There has been sporadic evidence, however, both historically and more recently, to indicate that the unit weight of soil water can greatly exceed 9.8 kN/m^3 in clayey soils at low water content. Values as high as 16.5 kN/m^3 have been reported (e.g., Martin 1960; Richards and Bouazza 2007) and more recent experimental evidence using helium gas pycnometer approaches (Zhang and Lu 2018a; Dong et al. 2020b) have further confirmed the pervasiveness of abnormally high soil water unit weight in clayey soils.

The recently developed soil sorptive potential theory (Lu and Zhang 2019) provided the quantitative theoretical and physical basis for why this is so. Water sorption on and within soil particles leads to extremely high compressive pressure (up to 1.6 GPa) adjacent to mineral surfaces (Lu and Khorshidi 2015; Khorshidi et al. 2016), leading to a soil water unit weight that can be significantly higher than that of free water (Zhang and Lu 2018a, b). Because sorptive potential is most significant for high-surface-area materials and at low gravimetric water content, its effects on soil water density are most pronounced under these conditions. For bentonite soils with specific surface area $>300\ \text{m}^2/\text{g}$, for example, the unit weight of soil water mostly exceeds 13.8 kN/m^3 for water content <15%, which is over 40% above the free water value of 9.8 kN/m^3 (Zhang and Lu 2018a, b).

Three practical questions arise: Is it necessary to consider soil water unit weight greater than the conventionally assumed value of 9.8 kN/m^3 in geotechnical and geoenvironmental practice? If so, how does the unit weight of soil water depend on water content, void ratio, and soil type? Finally, how can we practically account for these effects to accurately estimate the soil water unit weight for a wide range of soil types? We address these questions in the following by measuring soil water unit weight, soil water sorption isotherms, and soil shrinkage curves for various clayey and silty soils. Generalized soil phase relationships that account for variable soil water unit weight were derived. For soil under saturated conditions, the general phase relationships and experimental results were used to quantify void ratio as a function of the unit weight of soil water. For soil unsaturated conditions, the general phase relationships and experimental results were used to quantify degree of saturation as a function of the unit weight of soil water. Results are plotted in the form of practical charts that may be applied to a wide range of soil types.

---

[1] Research Associate, Dept. of Civil and Environmental Engineering, Univ. of Wisconsin-Madison, Madison, WI 53706; formerly, Postdoctoral Fellow, Dept. of Civil and Environmental Engineering, Colorado School of Mines, Golden, CO 80401. Email: shengminluo@mines.edu

[2] Professor, Henan Unsaturated Soil and Special Soil Engineering Technology Research Center, College of Architecture and Civil Engineering, Xinyang Normal Univ., Xinyang, Henan 464000, China. ORCID: https://orcid.org/0000-0002-9062-4102. Email: zhoubc@xynu.edu.cn

[3] Formerly, Ph.D. Candidate, Dept. of Civil and Environmental Engineering, Univ. of Massachusetts Amherst, Amherst, MA 01003. Email: jpeng@umass.edu

[4] Professor, Dept. of Civil and Environmental Engineering, Univ. of Wisconsin-Madison, Madison, WI 53706. Email: likos@wisc.edu

[5] Professor, Dept. of Civil and Environmental Engineering, Colorado School of Mines, Golden, CO 80401 (corresponding author). ORCID: https://orcid.org/0000-0003-1753-129X. Email: ninglu@mines.edu

Note. This manuscript was submitted on March 1, 2022; approved on October 25, 2022; published online on December 19, 2022. Discussion period open until May 19, 2023; separate discussions must be submitted for individual papers. This paper is part of the ***Journal of Geotechnical and Geoenvironmental Engineering***, © ASCE, ISSN 1090-0241.

J. Geotech. Geoenviron. Eng., 2023, 149(3): 04022134

Downloaded from ascelibrary.org by University of Wisconsin-Madison on 05/24/23. Copyright ASCE. For personal use only; all rights reserved.

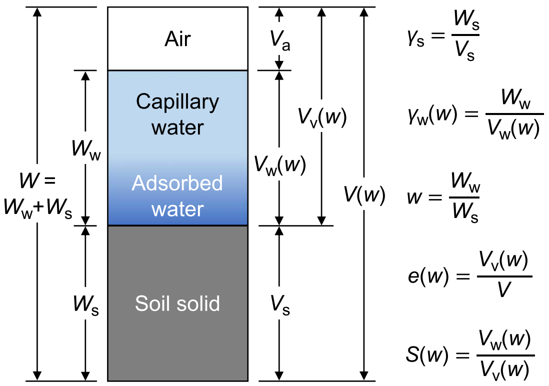

Fig. 1. Soil phase diagram under unsaturated conditions. The water phase is conceptually differentiated to include capillary water and adsorbed water owing to the presence of soil sorptive potential according to Lu and Zhang (2019).

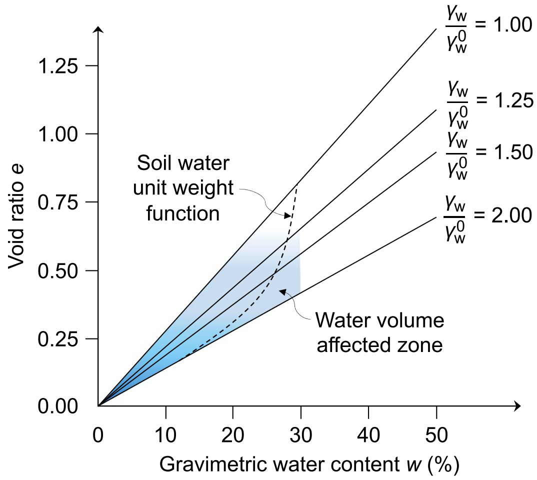

Fig. 2. Void ratio as a function of soil water content and soil water unit weight under the saturated condition. The water volume affected zone (shaded) indicates the influence of soil sorptive potential at low water content. The soil water unit weight function captures the dependency of soil water unit weight on void ratio and water content.

Soil Phase Relationships and Fundamental Soil Properties

General Soil Phase Diagram

Soil is a three-phase material consisting of air, liquid water, and soil solids. Weight–volume relationships among these phases are commonly represented using a soil phase diagram, as demonstrated in Fig. 1. Fundamental soil properties such as water content, void ratio, porosity, degree of saturation, and specific gravity are dictated and determined by the relative amount (mass or volume) of the different phases. A classic equation derived from the phase diagram to quantify the relationships among gravimetric water content (w), void ratio (e), degree of saturation (S), and specific gravity (G_s) is

$$Se = G_s w \tag{1}$$

where the underlying assumption in deriving Eq. (1) is that average soil water unit weight (γ_w) is equal to the unit weight of free water (γ_w^0), or $\gamma_w/\gamma_w^0 = 1$. Despite the prevalence of this assumption in practice, much higher unit weights have been reported in the literature (e.g., Martin 1960; Mitchell and Soga 2005). An upper bound of $1.872\ \mathrm{g/cm^3}$ for soil water density was estimated by Zhang and Lu (2018b), corresponding to unit weight of $18.3\ \mathrm{kN/m^3}$.

Void Ratio for Varying Water Unit Weight under Saturated Conditions

Eq. (1) can be rewritten in a more general form to consider the effect of variable soil water unit weight

$$\frac{\gamma_w}{\gamma_w^0} Se = G_s w \tag{2}$$

For a saturated soil, the degree of saturation (S) is equal to unity and Eq. (2) becomes

$$e = \frac{1}{\frac{\gamma_w}{\gamma_w^0}} G_s w \tag{3}$$

Considering Eq. (3), the influence of soil water unit weight on the relationship between void ratio and water content for constant G_s can be illustrated in Fig. 2 (assuming $G_s = 2.8$). The lower-bound ratio $\gamma_w/\gamma_w^0 = 1$ is the conventional case for soil water unit weight equal to $9.8\ \mathrm{kN/m^3}$, whereas the upper-bound ratio $\gamma_w/\gamma_w^0 = 2$ is the case when the soil water unit weight is $19.6\ \mathrm{kN/m^3}$ ($\gamma_w = 2.0\ \mathrm{g/cm^3}$), which may occur in expansive clays with water content less than 20% (e.g., De Wit and Arens 1950; Mooney et al. 1952; Baramian et al. 2017). In reality, the average water unit weight in soil is a monotonically decreasing function of water content with a lower-bound value of free water unit weight (Dong et al. 2020b; Martin 1960; Zhang and Lu 2018b). This results in dependency of the ratio $\gamma_w(w)/\gamma_w^0$ on soil water content, as illustrated by the dashed curve in Fig. 2. Higher soil water unit weight results in a decrease in void ratio at $S = 100\%$. The change in void ratio is most significant at relatively low soil water content and gradually diminishes as water content increases.

The relative change in void ratio can be obtained by taking the total differentiation of Eq. (3)

$$\frac{de}{e} = \frac{dw}{w} - \frac{1}{\gamma_w}\frac{d\gamma_w}{dw} dw \tag{4}$$

which indicates that an increase in soil water content results in an increase in void ratio through two mechanisms: (1) increases in soil water content (first term on the right-hand side of the equation); and (2) decreases in the rate of average soil water unit weight with respect to the increase in soil water content (second term on the right-hand side of the equation). The average soil water unit weight is defined as the ratio of total soil water mass to soil void volume. If the average soil water unit weight remains a constant of $9.8\ \mathrm{kN/m^3}$, the second term on the right-hand side becomes zero, and the relative change in void ratio is equal to the relative change in gravimetric water content.

Integrating Eq. (4) from the dry state at some initial void ratio e_0 ($e_0, w = 0$) to a state at some water content (e, w) leads to an expression for void ratio as a function of soil water content

$$e - e_0 = G_s \gamma_w^0 \left(\int_0^w \frac{1}{\gamma_w} dw - \int_0^w \frac{1}{\gamma_w^2} \frac{d\gamma_w}{dw} w dw \right) \tag{5}$$

Thus, if an analytical expression for soil water unit weight is available, or if experimental data for soil water unit weight are

Downloaded from ascelibrary.org by University of Wisconsin-Madison on 05/24/23. Copyright ASCE. For personal use only; all rights reserved.

available, then the void ratio as a function of soil water content can be fully established. Detailed derivation of Eqs. (4) and (5) is provided in the Appendix.

Degree of Saturation for Varying Water Unit Weight under Unsaturated Conditions

For soil under the unsaturated condition, the relationship among degree of saturation (S), gravimetric water content (w), and void ratio (e) for a varying soil water unit weight [$\gamma_w(w)$] is derived from Eq. (2) as follows:

$$S = \frac{1}{\frac{\gamma_w}{\gamma_w^0}} \frac{G_s w}{e} \tag{6}$$

Thus, if the soil water unit weight is greater than the free water unit weight in the low-water-content range (e.g., $w < 30\%$), the true degree of saturation is lower than the value calculated conventionally using a constant ratio $\gamma_w/\gamma_w^0 = 1$. In addition, if a soil deforms as the water content varies [i.e., $e(w)$], the change in degree of saturation can be derived by differentiating Eq. (6) (details provided in Appendix):

$$\mathrm{d}S = \frac{1}{\frac{\gamma_w}{\gamma_w^0}} \frac{G_s w}{e} \left(\frac{\mathrm{d}w}{w} - \frac{\mathrm{d}e}{e} - \frac{1}{\gamma_w} \frac{\mathrm{d}\gamma_w}{\mathrm{d}w} \mathrm{d}w \right) \tag{7}$$

The first term in the bracket of the right-hand side of Eq. (7) reflects an increase in degree of saturation due to an increase in water content. The second term reflects a decrease in the degree of saturation due swelling or an increase in the degree of saturation due to shrinkage of the soil. The third term reflects an increase in degree of saturation due to a decreasing rate in soil water unit weight as water content increases.

Experimental Methods and Database

One-Dimensional Consolidation

The preceding analysis indicated that the effects of variable soil water unit weight on soil phase relationships can be significant for clayey soils at low water content. It is thus important to experimentally quantify the effects of water content, void ratio, and soil type on the unit weight of soil water. According to the soil phase diagram (Fig. 1), the average water unit weight in soil (γ_w) is

$$\gamma_w = \frac{M_w}{V_w} = \frac{m_w}{V_w} g \tag{8}$$

where M_w and m_w = weight (N) and mass (kg) of soil water, respectively; V_w = volume of soil water (m^3); and g = gravitational acceleration (N/kg).

The mass and volume of soil water, and thus the corresponding soil water unit weight (Eq. 8), may be experimentally quantified using standard one-dimensional (1D) consolidation tests. Soil samples for the consolidation testing program herein were prepared following the specified procedures. Pulverized air-dried soil was sieved through a #40 sieve and dampened with deionized (DI) water to an initial gravimetric water content of 17%. Then, 23.60 g of the wet soil was filled into a consolidation ring with inner diameter of 39.1 mm and height of 10 mm using static load compaction, such that a soil cake with a dry density of 1.68 g/cm^3 was obtained. The compacted soil cake was transferred into a consolidation cell with porous stones and filter papers on the specimen's top and bottom surfaces (Fig. 3).

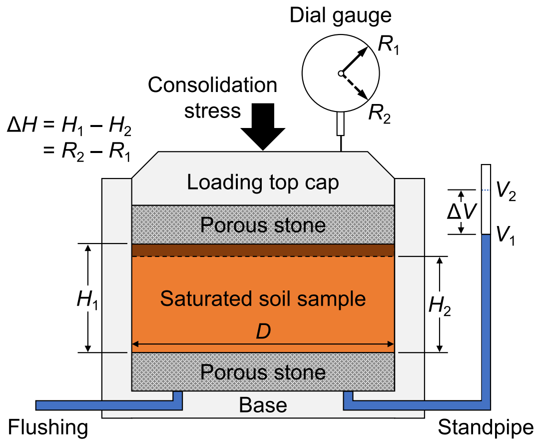

Fig. 3. Oedometer for measuring soil water density using a standard consolidation test.

The top loading cap was placed in position to ensure good contact between the surfaces. The consolidation cell enclosing the soil specimen was exposed to a vacuum pressure for at least 1 h followed by additional soaking in the vacuum chamber for 24 h to eliminate air bubbles entrained in the system [Lade 2016; ASTM D7370/D7370M-14 (ASTM 2021)]. Considering the relatively smaller dimensions of the soil cake (39.1-mm diameter and 10-mm height) used in this study than the common sample dimensions in oedometer testing, all specimens were thus assumed to be saturated during the consolidation tests. The height of the soil specimen was closely monitored throughout the process of preparation, and the total mass of the consolidation cell including the specimen was weighed upon completion of vacuum saturation.

All consolidation tests were conducted under the room temperature ranging between 21.2°C and 28.3°C, which could lead to soil water density variation within 0.998 − 0.996 g/cm^3 or relative ±0.1% variation with respect to the free water density of 0.997 g/cm^3 at 25.0°C. The initial soil water densities for all specimens were all very close to the standard 0.997 g/m^3 of the free water, calculated to be 0.996–1.000 g/cm^3 as shown in Fig. 4 for soil water unit weight range of 9.771–9.810 kN/m^3.

The consolidation cell containing the saturated soil specimen was installed on a high-capacity load frame (up to 12,000 kPa), and the water outlet port was connected to a high-resolution vertical standpipe for measuring the volume of water outflow from the bottom porous stone (Fig. 3). The drainage lines to the bottom of the specimen were flushed multiple times to evacuate entrapped air, and the flushing valve was then closed prior to an incremental-loading consolidation test. A loading schedule consisting of 10 increments from a minimum of 31.25 kPa to a maximum of 12,000 kPa (i.e., 12 MPa) was implemented. Except for the last stress level, the applied consolidation stress was doubled with each increment, leading to a load-increment ratio (LIR) of ~1.0 [ASTM D2435/D2435M-11 (ASTM 2020)]. Time-deformation readings were obtained during each increment using a dial gauge attached to the loading top cap and the volume of water expelled from the saturated sample was independently measured using the standpipe. Successive load increments were applied when there was no significant difference observed between consecutive readings on the dial gauge. The consolidation cell was covered with a watertight plastic membrane to suppress evaporation over the course of a

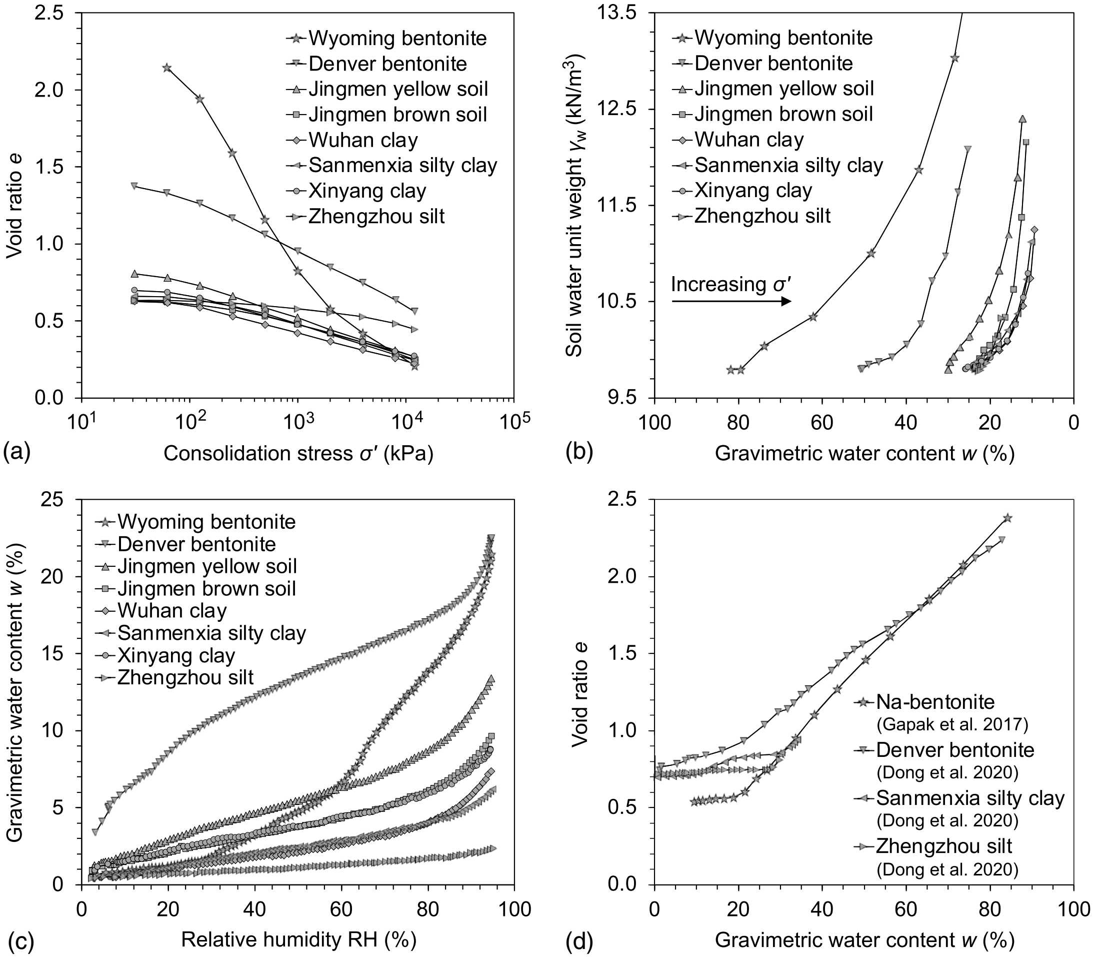

Fig. 4. Experimental results for various silty and clayey soils: (a) compression curves from 1D consolidation tests; (b) soil water unit weight functions; (c) adsorption paths of the soil water isotherms (data from Zhou and Lu 2021); and (d) soil shrinkage curves.

3-month testing period. The soil specimen was oven-dried at 105°C for 48 h at the end of the test to calculate the dry soil mass.

Determination of Soil Water Unit Weight Function

The soil water mass and soil water volume required to calculate soil water unit weight [Eq. (1)] may be obtained from the dial gauge and standpipe measurements. The volume of water drained during a specific loading increment was directly measured by the graduated standpipe (Fig. 3). Because the water collected in the standpipe is regarded as free water with known density, the mass of water expelled from the soil specimen from the beginning to the end of the ith increment ($m_{wd,i}$) is

$$m_{wd,i} = \rho_0 V_{wd,i} \tag{9}$$

where $V_{wd,i}$ = volume of expelled water collected by the standpipe. The water in the standpipe was under ambient atmospheric pressure and room temperature so its density ρ_0 was assumed to be $0.997\ \mathrm{g/cm^3}$. The mass of water retained by the soil at the end of the ith increment can be calculated based on conservation of mass as follows:

$$m_{w,i} = m_0 - m_s - \sum_1^i m_{wd,i} \tag{10}$$

where m_0 = total mass of the saturated soil sample measured immediately before the first loading increment; and m_s = mass of soil solids determined after oven-drying.

For 1D consolidation, the volume change of the soil specimen during the ith increment (V_i) was calculated based on the vertical displacement from the dial gauge

$$V_i = H_i A_0 = H_i \frac{\pi D^2}{4} \tag{11}$$

where H_i = change in specimen height during the ith increment; A_0 = area of the specimen; and D = diameter of the specimen.

The bulk volume change of the specimen (V_i) and the volume of water collected by the standpipe ($V_{wd,i}$) are not necessarily equal because the water in the specimen transitions from soil water to free water, which can be accompanied by a density change. As such, the volume of water remaining in soil at the end of the ith increment must be determined indirectly as follows:

$$\begin{aligned} V_{w,i} &= V_0 - \sum_1^i V_i - V_s = \left(H_0 - \sum_1^i H_i\right) A_0 - V_s \\ &= \left(H_0 - \sum_1^i H_i\right) \frac{\pi D^2}{4} - V_s \end{aligned} \tag{12}$$

where V_0 and H_0 = total volume and initial height of the saturated soil sample measured immediately before the first loading

Downloaded from ascelibrary.org by University of Wisconsin-Madison on 05/24/23. Copyright ASCE. For personal use only; all rights reserved.

increment; and V_s = volume of soil solid. The latter is a constant and can be determined as follows:

$$V_s = \frac{m_s}{\rho_s} = \frac{m_s}{G_s \rho_0} \tag{13}$$

Substituting Eqs. (3), (5), and (6) into Eq. (1), the average soil water unit weight at the end of the ith increment ($\gamma_{w,i}$) is calculated as follows:

$$\gamma_{w,i} = \frac{m_{w,i}}{V_{w,i}} g = 4 G_s \rho_0 g \frac{m_0 - m_s - \sum_1^i m_{wd,i}}{G_s \rho_0 \pi D^2 (H_0 - \sum_1^i H_i) - 4 m_s} \tag{14}$$

and the corresponding soil water content (w_i) is

$$w_i = \frac{m_{w,i}}{m_s} = \frac{m_0 - m_s - \sum_1^i m_{wd,i}}{m_s} \tag{15}$$

The soil water unit weight can thus be characterized as a function of soil water content $\gamma_w(w)]$ at different stress levels throughout the consolidation test.

Experimental Database

Eight soils, including low-plasticity silty soils and high-plasticity clayey soils, were selected to determine soil water unit weight functions using the consolidation procedures described previously. Soils were selected to represent a variety of fine-grained soils based on their basic geotechnical index properties (e.g., Atterberg limits) and soil classification, as summarized in Table 1.

Soil water isotherms (SWI) describing the relationship between gravimetric water content and relative humidity (RH) were measured for the same soils by Zhou and Lu (2021) using a vapor sorption analyzer (Meter Group, Pullman, Washington) at 25°C (Likos et al. 2011). The full wetting-drying loop for a SWI measured using this approach typically includes 200 discrete measurements for RH ranging from 3% to 95%. Here, only the wetting path was obtained and used to determine the fundamental soil physical properties total specific surface area (SSA) following procedures described by Lu and Zhang (2020). Cation exchange capacity (CEC) values for the soils were obtained using the ammonium displacement method [ASTM D7503 (ASTM 2010)], as reported by Zhou and Lu (2021). The total SSA of the eight soils ranged from 26 $\mathrm{m^2/g}$ (Zhengzhou silt) to 600 $\mathrm{m^2/g}$ (Wyoming bentonite), and CEC ranged from 5 cmol/kg (Zhengzhou silt) to 98 cmol/kg (Denver bentonite) (Table 1).

Soil shrinkage curves (i.e., void ratio versus water content) for four soils (Zhengzhou silt, Sanmenxia silty clay, Denver bentonite, and Na-bentonite) were obtained to investigate how bulk volume changes, together with the varying soil water unit weight, affected soil degree of saturation under the unsaturated condition. Shrinkage curves for the first three soils were obtained previously (Dong et al. 2020a) and are the same soils as those tested here for 1D consolidation. The shrinkage curve for the fourth soil was reported by Gapak et al. (2017) and is a sodium bentonite (labeled B4) with composition, consistency limits, SSA, and CEC similar to the Wyoming bentonite examined in this study.

Experimental Results

Soil Water Unit Weight Function

Compression curves for the eight soils measured by consolidation testing are shown in Fig. 4(a). In each case, at least two-thirds of the initial soil volume was compressed after completion of the last loading increment of 12 MPa. Corresponding soil water unit weight functions [Fig. 4(b) and Table 2] showed an increasing trend with increasing consolidation stress level (or decreasing soil water content).

This general trend is interpreted as follows. Soil water exists mainly in two forms (Fig. 1): capillary water retained primarily in relatively large pores and adsorbed water retained primarily in relatively small pores adjacent to mineral surfaces (e.g., Frydman and Baker 2009). For a saturated soil with zero external load, capillary water has a unit weight identical with free water. Adsorbed water has a unit weight greater than free water resulting from the adsorption-induced compressive pressure (Zhang and Lu 2018b). Capillary water is preferentially expelled during consolidation due to its higher mobility than the adsorbed water, which leads to a continuous increase in the volume fraction of adsorbed water remaining in the soil, and hence an increase in average soil water unit weight [Fig. 4(b)].

Fig. 4(b) also shows that average soil water unit weights in clayey soils generally deviated more from that of free water than in silty soils, indicating a dependence of soil water unit weight on soil type. For example, except for Zhengzhou silt, the soil water unit weight functions mostly exceeded 10.8 $\mathrm{kN/m^3}$ (10% higher than free water unit weight) at the 12-MPa consolidation stress; however, the water unit weight in Wyoming bentonite reached 10.8 $\mathrm{kN/m^3}$ at a much lower consolidation stress of 500 kPa (corresponding to water content of 48%).

The influence of soil physical properties on soil water unit weight can be inferred from the soil water isotherms [Fig. 4(c)]. The maximum water content for the measured isotherm data obtained at RH of 95% ranged from 2.3% (Zhengzhou silt) to 22.5% (Denver bentonite). Higher maximum water content generally indicates a finer or higher-surface-area soil with stronger

Table 1. Geotechnical and physical properties of eight soils

Soil name	LL (%)	PL (%)	PI	USCS	G_s	Total SSA ($\mathrm{m^2/g}$)	CEC (cmol/kg)	Swelling potential[a]
Zhengzhou silt	26	15	11	CL	2.70	26	5	Low
Sanmenxia silty clay	35	19	16	CL	2.72	110	15	Medium
Jingmen brown soil	42	21	21	CL	2.72	144	25	High
Wuhan clay	40	18	22	CL	2.73	94	15	High
Xinyang clay	42	19	23	CL	2.72	114	21	High
Jingmen yellow soil	63	26	37	CH	2.75	251	31	Very high
Denver bentonite	104	48	56	MH	2.73	566	98	Very high
Wyoming bentonite	218	33	185	CH	2.70	600	62	Very high

Note: LL = liquid limit; PL = plastic limit; PI = plasticity index; USCS = unified soil classification system; CL = low plasticity clay; CH = high plasticity clay; and MH = high plasticity silt.

[a] By Chen's (1988) expansive soil classification.

Downloaded from ascelibrary.org by University of Wisconsin-Madison on 05/24/23. Copyright ASCE. For personal use only; all rights reserved.

Downloaded from ascelibrary.org by University of Wisconsin-Madison on 05/24/23. Copyright ASCE. For personal use only; all rights reserved.

Table 2. Summary of soil water unit weight function inferred from incremental loading consolidation test

Soil name	Soil water unit weight function	Consolidation stress (kPa) 0	31.25	62.5	125	250	500	1,000	2,000	4,000	8,000	12,000
Zhengzhou silt	w (%)	23.5	23.5	23.5	23.3	22.7	22.2	21.5	20.7	19.8	18.5	17.4
	γ_w (kN/m^3)	9.8	9.8	9.8	9.8	9.8	9.8	9.8	9.9	9.9	10.1	10.3
Sanmenxia silty clay	w (%)	24.4	24.4	24.3	23.5	22.1	20.5	18.1	15.8	13.5	11.3	10.2
	γ_w (kN/m^3)	9.8	9.8	9.8	9.9	9.9	10.0	10.1	10.2	10.4	10.7	11.1
Jingmen brown soil	w (%)	23.4	23.2	23.0	22.4	21.4	20.0	18.2	16.3	14.4	12.5	11.4
	γ_w (kN/m^3)	9.8	9.8	9.8	9.9	10.0	10.0	10.1	10.3	10.6	11.4	12.2
Wuhan clay	w (%)	23.2	23.0	22.8	21.7	19.7	17.8	15.9	14.1	12.2	10.4	9.4
	γ_w (kN/m^3)	9.8	9.8	9.8	9.9	10.0	10.0	10.1	10.3	10.5	10.7	11.3
Xinyang clay	w (%)	25.8	25.7	25.3	24.0	22.0	19.9	17.9	15.9	14.0	12.0	10.9
	γ_w (kN/m^3)	9.8	9.8	9.8	9.8	9.9	9.9	10.0	10.1	10.3	10.5	10.8
Jingmen yellow soil	w (%)	30.0	29.5	28.7	27.2	24.9	22.5	20.4	17.8	15.7	13.6	12.3
	γ_w (kN/m^3)	9.8	9.9	9.9	10.0	10.1	10.3	10.5	10.8	11.2	11.8	12.4
Denver bentonite	w (%)	50.7	50.3	48.9	46.5	43.3	39.8	36.6	33.9	30.7	27.7	25.3
	γ_w (kN/m^3)	9.8	9.8	9.8	9.9	9.9	10.1	10.3	10.7	11.0	11.6	12.1
Wyoming bentonite	w (%)	81.7	—	79.3	73.7	62.2	48.2	37.0	28.5	22.9	18.0	15.2
	γ_w (kN/m^3)	9.8	—	9.8	10.0	10.4	11.0	11.9	13.0	14.4	16.4	18.8

capacity for water adsorption, which is consistent with the pattern observed for the soil water unit weight functions in Fig. 4(b).

Error Assessments in Using Constant Soil Water Unit Weight

A constant unit weight of water (i.e., 9.8 kN/m^3) has been invariably assumed and used in almost any case of geotechnical and geoenvironmental engineering for conversion between weight and volume of soil water. A unit weight of soil water higher than that of free water, as observed in Fig. 4(b), can thus produce error in calculation of water volume from water weight (or vice versa), resulting in unreasonable physical properties determined therefrom (e.g., $S > 100\%$) (e.g., Villar and Lloret 2004).

Fig. 5 visually demonstrates how and to what extent a variable soil water unit weight affects the volume of each phase for two specific soils (Sanmenxia silty clay and Jingmen yellow soil) under saturated conditions. No air is present under saturated conditions and water occupies all void space. For the same volume of soil solid (V_s), the volume of water (V_w) can be determined using specific gravity (G_s), gravimetric water content (w), and soil water unit weight (γ_w).

For two soils with similar water content, Fig. 5 compares the difference between soil water volumes calculated from the free water unit weight ($\gamma_w^0 = 9.8$ kN/m^3) and from the actual average soil water unit weight (γ_w) inferred from consolidation testing. The water volume was overestimated in both cases. If the inferred soil water unit weight was used, the soil water volume was reduced by 3.94% for Sanmenxia silty clay and 12.43% for Jingmen yellow soil. Even though these two soils have almost identical water content, the relative error in estimating the soil water volume caused by the variation in soil water unit weight was three times higher in the Jingmen yellow soil than the Sanmenxia silty clay. This reflects the generally stronger soil sorptive potential in clayey soils than silty soils (Zhang and Lu 2020).

For soils under the unsaturated condition, the relative difference in water volume between free water and soil water can be calculated

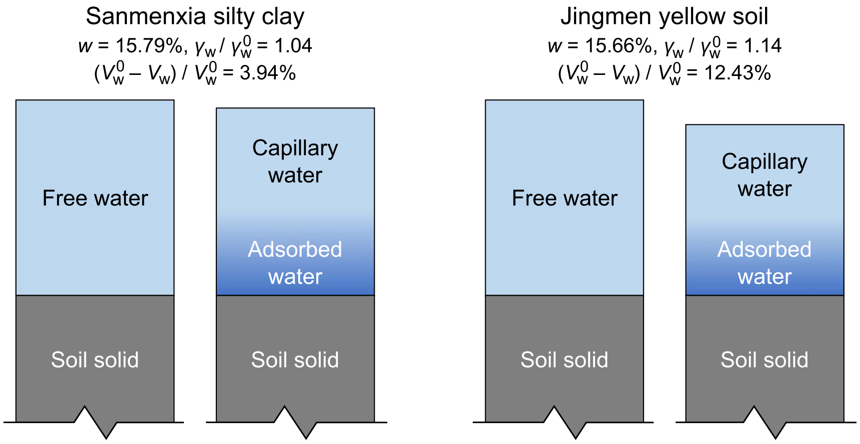

Fig. 5. Relative difference in soil water volume estimation due to the variation of soil water unit weight for saturated silty and clayey soils. The height of each rectangle represents the volume of each phase.

Downloaded from ascelibrary.org by University of Wisconsin-Madison on 05/24/23. Copyright ASCE. For personal use only; all rights reserved.

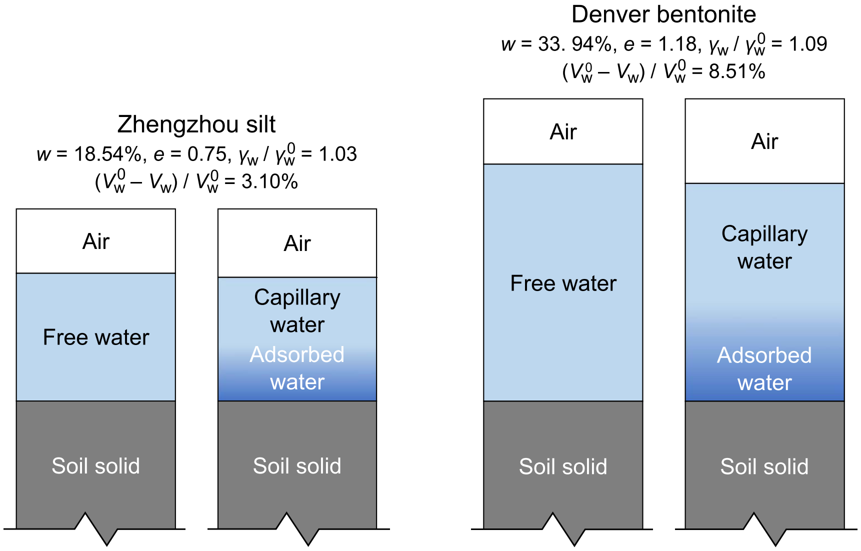

Fig. 6. Relative difference in soil water volume estimation due to the variation of soil water unit weight for unsaturated silty and clayey soils. The height of each rectangle represents the volume of each phase.

following the same procedures. Fig. 6 illustrates phase diagrams for a silty soil (Zhengzhou silt) and a swelling clay (Denver bentonite). The water volume for Zhengzhou silt at water content of 18.54% was overestimated by 3.10% if free water unit weight is used, whereas an error of 8.51% will be introduced in Denver bentonite even at a much higher water content of 33.94%.

The effects of overestimating soil water volume on the determination of void ratio (saturated condition) and degree of saturation (unsaturated condition) can be quantified via Eqs. (3) and (6), respectively. For instance, the absolute error in void ratio due to variation of soil water unit weight is calculated as follows:

$$e^0 - e = G_s w - \frac{1}{\frac{\gamma_w}{\gamma_w^0}} G_s w = G_s w \left(1 - \frac{1}{\frac{\gamma_w}{\gamma_w^0}}\right) \tag{16}$$

and the relative error becomes

$$\frac{e^0 - e}{e^0} = 1 - \frac{1}{\frac{\gamma_w}{\gamma_w^0}} \tag{17}$$

These two quantities can be determined if the soil water unit weight function $[\gamma_w(w)]$ is defined. Similar expressions for absolute and relative error in degree of saturation are as follows:

$$S^0 - S = \frac{G_s w}{e} - \frac{1}{\frac{\gamma_w}{\gamma_w^0}} \frac{G_s w}{e} = \frac{G_s w}{e} \left(1 - \frac{1}{\frac{\gamma_w}{\gamma_w^0}}\right) \tag{18}$$

$$\frac{S^0 - S}{S^0} = 1 - \frac{1}{\frac{\gamma_w}{\gamma_w^0}} \tag{19}$$

Determination of absolute difference in degree of saturation requires both the soil water unit weight function $[\gamma_w(w)]$ and the soil shrinkage curve $[e(w)]$. The soil water unit weight function determined from the saturated consolidation test was assumed applicable to the unsaturated condition. A constant void ratio (i.e., nondeformable soil frame) of 1.0 was also assumed here for the four soils (i.e., Jingmen yellow soil, Jingmen brown soil, Wuhan clay, and Xinyang clay) whose soil shrinkage curves (SSC) were not available.

Fig. 7 shows results for absolute and relative error in void ratio and degree of saturation. The highest absolute error in void ratio (i.e., 0.2) was found for the Wyoming bentonite at a water content range of 20%–30%, whereas Zhengzhou silt provided the lowest error in the void ratio (0.02) at water content of 17% [Fig. 7(a)]. Except for the two highly swelling clays (i.e., Wyoming bentonite and Denver bentonite), the effect of varying water unit weight will only be significant for most soils when the gravimetric water content is below 30%.

The highest absolute error in degree of saturation among the different soils ranged from 3% to 35% [Fig. 7(c)], increasing from silty soils (e.g., Sanmenxia silty clay and Zhengzhou silt) to clayey soils (e.g., Jingmen yellow soil and Jingmen brown soil) and finally to the swelling clays (Wyoming bentonite and Denver bentonite). However, the two plots for relative errors in void ratio [Fig. 7(b)] and degree of saturation [Fig. 7(d)] are identical because the relative error is completely controlled by the soil water unit weight function [Eqs. (17) and (19)], no matter whether void ratio or degree of saturation is considered. Although the relative error calculated for silty soils barely exceeded 10%, most clayey soils at water content less than 15% will show a relative error between 15% and 20%. Swelling bentonite clays ramped up the relative error to 30% even at a relatively high water content of 30%.

Intrinsic Relationships between Soil Water Unit Weight and Soil Properties

Compressive water pressure induced by water adsorption in fine-grained soil is the main mechanism that increases the soil water unit weight above that of free water (Lu et al. 2022). The average soil water unit weight for each soil in Fig. 4(b) invariably increased with decreasing water content. This is because large pores in soil during consolidation are gradually compressed into smaller ones in which water adsorption prevails. The soil water unit weight function was also found to vary greatly among soils, depending primarily on the soil type. Contour plots (Fig. 8) for soil water unit weight were generated and smoothed (MATLAB version 2019a) based on the soil water unit weight functions inferred from the consolidation test [Fig. 4(b)]. Fig. 8(a) illustrates that the unit weight of soil water increased with increasing liquid limit and

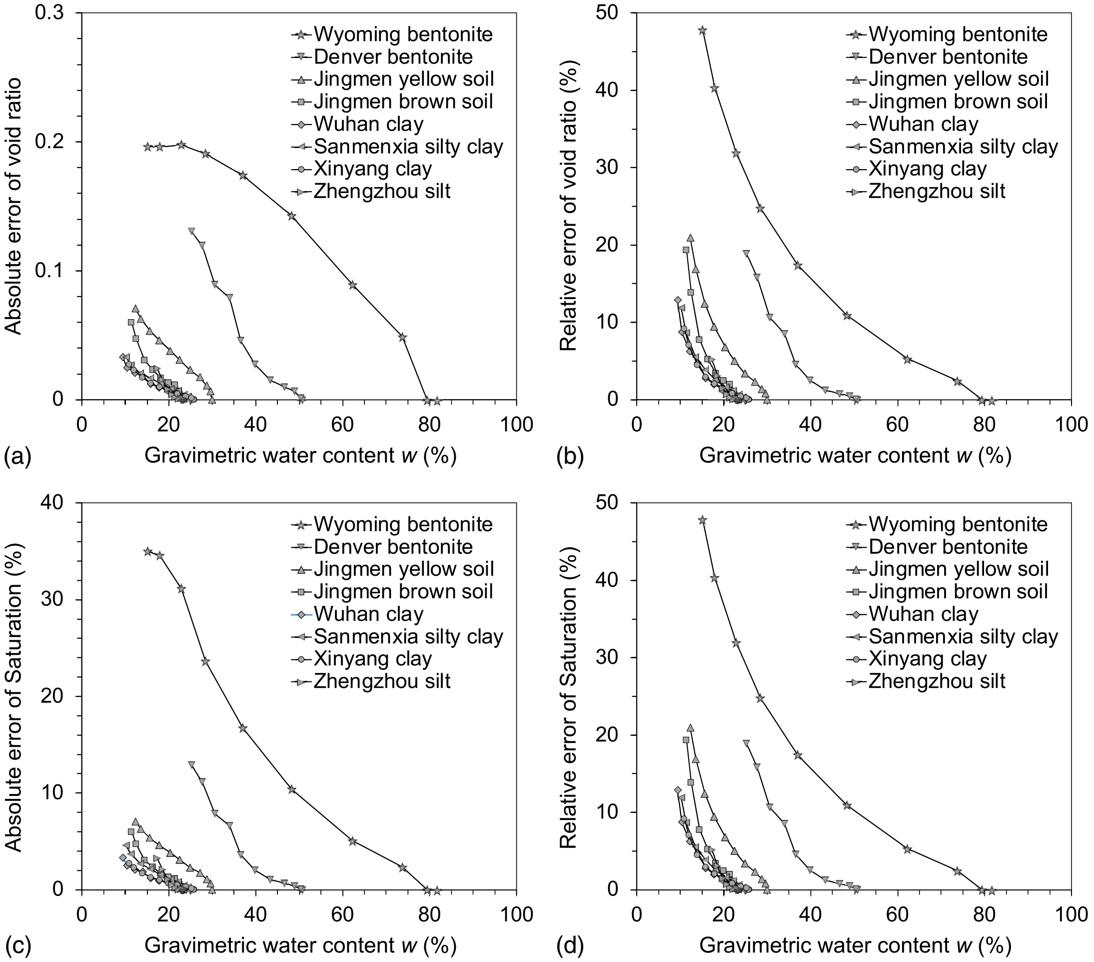

Fig. 7. For various silty and clayey soils, results of (a and b) absolute and relative error of void ratio as a function of soil water content under the saturated condition; and (c and d) absolute and relative error of saturation as a function of soil water content under the unsaturated condition.

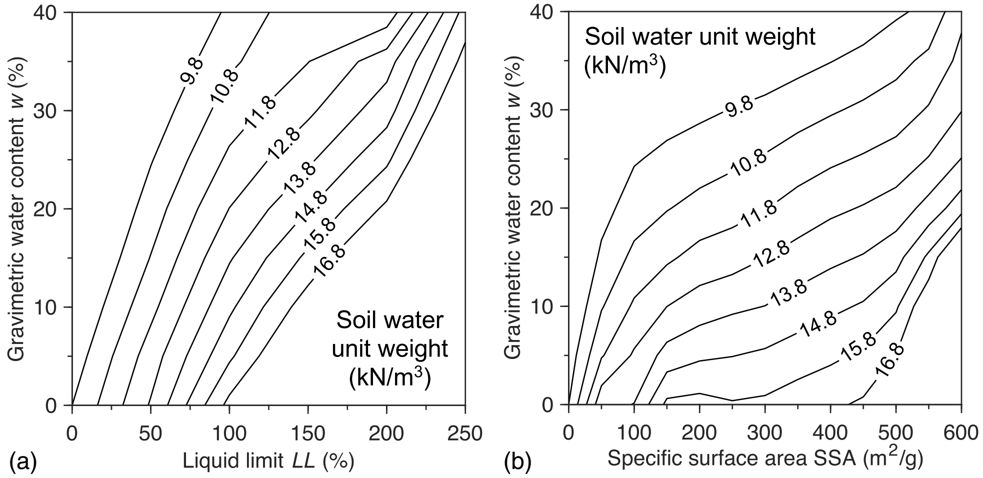

Fig. 8. Contours of soil water unit weight as a function of (a) liquid limit and gravimetric water content; and (b) specific surface area and gravimetric water content.

decreasing soil water content under the isothermal condition. This is consistent with the notion that the effect of adsorbed water on soil water unit weight is more significant in high-plasticity clayey soils than in silty soils.

Fig. 8(b) is a similar contour plot for soil water unit weight in the space of SSA and water content. Because SSA is an intrinsic soil property that plays a fundamental role in governing the Atterberg limits (i.e., liquid and plastic limits) of soil (e.g., Zhou and Lu 2021),

Downloaded from ascelibrary.org by University of Wisconsin-Madison on 05/24/23. Copyright ASCE. For personal use only; all rights reserved.

Downloaded from ascelibrary.org by University of Wisconsin-Madison on 05/24/23. Copyright ASCE. For personal use only; all rights reserved.

Table 3. Variation of soil water unit weight $\gamma_w(\mathrm{kN/m^3})$ with gravimetric water content and liquid limit

Gravimetric water content, w (%)	Liquid limit, LL (%)					
	0	50	100	150	200	250
0	9.8	12.9	17.1	19.9	23.7	28.0
5	9.8	12.3	15.6	18.8	22.1	26.3
10	9.8	11.5	14.6	17.4	20.3	24.5
15	9.8	10.8	13.7	16.0	18.6	22.8
20	9.8	10.3	12.8	14.8	17.0	21.1
25	9.8	9.8	12.0	13.6	15.6	19.6
30	9.8	9.8	11.3	12.6	14.4	18.3
35	9.8	9.8	10.6	11.8	13.4	17.2
40	9.8	9.8	9.9	11.6	11.1	16.2

soil with a higher SSA provides a larger amount of surface to adsorb water. This leads to higher water unit weight in clayey soils (e.g., Wyoming bentonite and Denver bentonite) than silty soils (e.g., Zhengzhou silt and Sanmenxia silty clay) at the same water content [Fig. 4(b)]. For soils with SSA of 150 $\mathrm{m^2/g}$, the soil water unit weight exceeded 10.8 $\mathrm{kN/m^3}$ at a gravimetric water content lower than 20%, which is 10% higher than the commonly used free water unit weight of 9.8 $\mathrm{kN/m^3}$. For swelling clays with SSA greater than 300 $\mathrm{m^2/g}$, the soil water unit weight mostly exceeded 12.8 $\mathrm{kN/m^3}$ at water content lower than 15%, which is about 31% higher than 9.8 $\mathrm{kN/m^3}$. Although the water unit weight in silty soils (e.g., SSA <50 $\mathrm{m^2/g}$) only deviated significantly from the free water unit weight at very low water content (e.g., $w < 5\%$), the variation of water unit weight in clayey soils need to be considered, as quantitatively evaluated in the preceding paragraphs. To make Fig. 8 more convenient for practical applications, Tables 3 and 4 present two readily implementable charts that digitize the contour plots displayed in Fig. 8. Soil water unit weight can be easily determined by linear interpolation based on soil water content and liquid limit or SSA.

Summary and Conclusions

A constant soil water unit weight of 9.8 $\mathrm{kN/m^3}$ has been conventionally considered for determination of basic soil phase relations such as void ratio and saturation. Experimental evidence and theoretical studies have indicated that the water unit weight in soil can be significantly greater than that of free water and depends primarily on soil type and the volume scale with which it is defined. Soil water unit weight can be measurably above 9.8 $\mathrm{kN/m^3}$ for clayey soils at less than 30% gravimetric water content, leading to unrealistic predictions of soil properties (e.g., degree of saturation greater than 100%) if a constant water unit weight for free water is assumed.

Incremental-loading consolidation tests were used to infer soil water unit weight as a function of soil water content. A wide variety of soils were covered by the testing program, including both low-plasticity silty soils and high-plasticity clayey soils. Average soil water unit weight increased above 9.8 $\mathrm{kN/m^3}$ as soil water content decreased with increasing consolidation stress. For highly expansive soil (Wyoming bentonite), the average soil water unit weight can be as high as 18.8 $\mathrm{kN/m^3}$ for gravimetric water content less than 18%. For clayey soils with lower liquid limit, the average soil water unit weight can be as high as 12.5 $\mathrm{kN/m^3}$ for gravimetric water content less than 10%.

The effect of a variable soil water unit weight function on quantifying soil phase volumes, void ratio, and saturation was experimentally assessed and theoretically interpreted as a function of soil water content and soil type. The analysis demonstrated that the liquid-phase volume can be overestimated as much as 48% if soil water unit weight of 9.8 $\mathrm{kN/m^3}$ is used, leading to overestimation of void ratio as high as 0.2 (absolute error) and degree of saturation as much as 35.0% (absolute difference). Based on the experimental soil water unit weight data, two charts were generated for general practical application of a variable soil water unit weight function. One chart provides relations among average soil water unit weight as a function of soil water content and liquid limit. A second chart provides relations among average soil water unit weight as a function of soil water content and soil specific surface area. It is concluded that the commonly adopted constant of 9.8 $\mathrm{kN/m^3}$ for water unit weight can lead to errors in estimating soil void ratio and degree of saturation for silty and clayey soils.

Appendix. Change in Phase Volume due to Soil Water Unit Weight Variation

Void Ratio for Saturated Condition

Eq. (3) can be rearranged as follows:

$$e = \gamma_w^0 G_s \frac{w}{\gamma_w} \tag{20}$$

Because both void ratio (e) and soil water unit weight (γ_w) are the functions of soil water content (w), the total derivative of void ratio is

Table 4. Variation of soil water unit weight $\gamma_w(\mathrm{kN/m^3})$ with gravimetric water content and specific surface area

Gravimetric water content, w (%)	Specific surface area, SSA ($\mathrm{m^2/g}$)												
	0	50	100	150	200	250	300	350	400	450	500	550	600
0	9.8	13.5	13.8	16.0	16.1	15.9	16.0	16.3	16.6	17.0	17.5	18.8	25.6
5	9.8	11.7	12.9	14.2	14.6	14.8	15.0	15.3	15.6	16.0	16.8	19.0	23.7
10	9.8	10.7	12.0	12.8	13.3	13.6	13.8	14.2	14.6	14.9	15.7	17.8	21.6
15	9.8	10.0	11.0	11.6	12.2	12.4	12.8	13.2	13.6	13.9	14.4	16.0	18.9
20	9.8	9.8	10.3	10.7	11.1	11.4	11.8	12.2	12.6	12.9	13.2	14.2	15.4
25	9.8	9.8	9.8	10.0	10.3	10.6	10.9	11.3	11.6	11.9	12.2	12.9	13.8
30	9.8	9.8	9.8	9.8	9.8	9.8	10.1	10.4	10.7	11.0	11.3	11.9	12.8
35	9.8	9.8	9.8	9.8	9.8	9.8	9.8	9.8	9.8	10.1	10.5	11.0	12.1
40	9.8	9.8	9.8	9.8	9.8	9.8	9.8	9.8	9.8	9.8	9.8	10.0	11.6

Downloaded from ascelibrary.org by University of Wisconsin-Madison on 05/24/23. Copyright ASCE. For personal use only; all rights reserved.

$$\begin{aligned}\mathrm{d}e &= \gamma_w^0 G_s\left[\frac{\gamma_w - w(\mathrm{d}\gamma_w/\mathrm{d}w)}{\gamma_w^2}\right]\mathrm{d}w \\ &= \gamma_w^0 G_s\left[\frac{1}{\gamma_w} - \frac{w(\mathrm{d}\gamma_w/\mathrm{d}w)}{\gamma_w^2}\right]\mathrm{d}w \\ &= \frac{\gamma_w^0 G_s}{\gamma_w}\mathrm{d}w - \frac{\gamma_w^0 G_s w(\mathrm{d}\gamma_w/\mathrm{d}w)}{\gamma_w^2}\mathrm{d}w \end{aligned} \tag{21}$$

Substituting Eq. (21) into Eq. (20) leads to:

$$\mathrm{d}e = \frac{e}{w}\mathrm{d}w - \frac{e}{\gamma_w}\frac{\mathrm{d}\gamma_w}{\mathrm{d}w}\mathrm{d}w \tag{22}$$

Eq. (4) is then obtained by rearranging Eq. (22), and integrating Eq. (21) yields

$$\int_{e_0}^{e}\mathrm{d}e = \int_0^w \gamma_w^0 G_s\left[\frac{1}{\gamma_w} - \frac{w(\mathrm{d}\gamma_w/\mathrm{d}w)}{\gamma_w^2}\right]\mathrm{d}w \tag{23}$$

Thus, Eq. (5) is derived as follows:

$$\begin{aligned}e - e_0 &= G_s\gamma_w^0\int_0^w\left[\frac{1}{\gamma_w} - \frac{w(\mathrm{d}\gamma_w/\mathrm{d}w)}{\gamma_w^2}\right]\mathrm{d}w \\ &= G_s\gamma_w^0\left(\int_0^w\frac{1}{\gamma_w}\mathrm{d}w - \int_0^w\frac{1}{\gamma_w^2}\frac{\mathrm{d}\gamma_w}{\mathrm{d}w}w\mathrm{d}w\right)\end{aligned} \tag{24}$$

Degree of Saturation for Unsaturated Condition

The change in degree of saturation (S) is calculated by taking the total derivative of Eq. (6)

$$\begin{aligned}\mathrm{d}S &= \frac{\partial S}{\partial e}\mathrm{d}e + \frac{\partial S}{\partial w}\mathrm{d}w = \frac{\gamma_w^0 G_s}{\gamma_w}\left(-\frac{w}{e^2}\right)\mathrm{d}e \\ &\quad + \frac{\gamma_w^0 G_s}{e}\left[\frac{\gamma_w - w(\mathrm{d}\gamma_w/\mathrm{d}w)}{\gamma_w^2}\right]\mathrm{d}w \\ &= -\frac{\gamma_w^0 G_s w}{\gamma_w e^2}\mathrm{d}e + \frac{\gamma_w^0 G_s}{e}\left[\frac{1}{\gamma_w} - \frac{w(\mathrm{d}\gamma_w/\mathrm{d}w)}{\gamma_w^2}\right]\mathrm{d}w \\ &= -\frac{\gamma_w^0 G_s w}{\gamma_w e^2}\mathrm{d}e + \frac{\gamma_w^0 G_s}{\gamma_w e}\mathrm{d}w - \frac{\gamma_w^0 G_s}{\gamma_w^2 e}\frac{\mathrm{d}\gamma_w}{\mathrm{d}w}w\mathrm{d}w \\ &= \frac{\gamma_w^0 G_s w}{\gamma_w e}\left(-\frac{\mathrm{d}e}{e} + \frac{\mathrm{d}w}{w} - \frac{1}{\gamma_w}\frac{\mathrm{d}\gamma_w}{\mathrm{d}w}\mathrm{d}w\right)\end{aligned} \tag{25}$$

Eq. (7) can be obtained by simplifying Eq. (25).

Data Availability Statement

All data, models, and code generated or used during the study appear in the published article.

Acknowledgments

This research is supported by the US National Science Foundation (NSF CMMI-1902045 and NSF CMMI-1902008) and National Natural Science Foundation of China (NSFC 11772290). Assistance from Mr. Yuzhe Yan, Mr. Lei Zhao, and Mr. Xianda Yi for the consolidation tests is greatly appreciated.

References

ASTM. 2010. *Standard test method for measuring exchange complex and cation exchange capacity of inorganic fine-grained soils*. ASTM D7503. West Conshohocken, PA: ASTM.

ASTM. 2020. *Standard test methods for one-dimensional consolidation properties of soils using incremental loading*. ASTM D2435/D2435M-11. West Conshohocken, PA: ASTM.

ASTM. 2021. *Standard test method for determination of relative density and absorption of fine, coarse, and blended aggregate using combined vacuum saturation and rapid submersion*. ASTM D7370/D7370M-14. West Conshohocken, PA: ASTM.

Bahramian, Y., A. Bahramian, and A. Javadi. 2017. "Confined fluids in clay interlayers: A simple method for density and abnormal pore pressure interpretation." *Colloids Surf., A* 521 (May): 260–271. https://doi.org/10.1016/j.colsurfa.2016.08.021.

De Wit, C. T., and P. L. Arens. 1950. "Moisture content and density of some clay minerals and some remarks on the hydration pattern of clay." In *Proc., 4th Int. Congress of Soil Science Transactions*, 59–62. Groningen, Netherlands: Hoitesema Brothers.

Dong, Y., N. Lu, and P. J. Fox. 2020a. "Drying-induced consolidation in soil." *J. Geotech. Geoenviron. Eng.* 146 (9): 4020092. https://doi.org/10.1061/(ASCE)GT.1943-5606.0002327.

Dong, Y., C. Wei, and N. Lu. 2020b. "Identifying soil adsorptive water by soil water density." *J. Geotech. Geoenviron. Eng.* 146 (7): 2820001. https://doi.org/10.1061/(ASCE)GT.1943-5606.0002289.

Frydman, S., and R. Baker. 2009. "Theoretical soil-water characteristic curves based on adsorption, cavitation, and a double porosity model." *Int. J. Geomech.* 9 (6): 250–257. https://doi.org/10.1061/(ASCE)1532-3641(2009)9:6(250).

Gapak, Y., G. Das, U. Yerramshetty, and T. V. Bharat. 2017. "Laboratory determination of volumetric shrinkage behavior of bentonites: A critical appraisal." *Appl. Clay Sci.* 135 (5): 554–566. https://doi.org/10.1016/j.clay.2016.10.038.

Khorshidi, M., N. Lu, and A. Khorshidi. 2016. "Intrinsic relationship between matric potential and cation hydration." *Vadose Zone J.* 15 (11): 1. https://doi.org/10.2136/vzj2016.01.0001.

Lade, P. V. 2016. "Specimen saturation." In *Triaxial testing of soils*. Hoboken, NJ: Wiley.

Likos, W. J., N. Lu, and W. Wensel. 2011. "Performance of a dynamic dew point method for moisture isotherms of clays." *Geotech. Test. J.* 34 (4): 373–382. https://doi.org/10.1520/GTJ102901.

Lu, N., and M. Khorshidi. 2015. "Mechanisms for soil-water retention and hysteresis at high suction range." *J. Geotech. Geoenviron. Eng.* 141 (8): 4015032. https://doi.org/10.1061/(ASCE)GT.1943-5606.0001325.

Lu, N., S. Luo, and B. Zhou. 2022. "Water adsorption-induced pore water pressure in soil." *J. Geotech. Geoenviron. Eng.* 148 (6): 04022042. https://doi.org/10.1061/(ASCE)GT.1943-5606.0002814.

Lu, N., and C. Zhang. 2019. "Soil sorptive potential: Concept, theory, and verification." *J. Geotech. Geoenviron. Eng.* 145 (4): 4019006. https://doi.org/10.1061/(ASCE)GT.1943-5606.0002025.

Lu, N., and C. Zhang. 2020. "Separating external and internal surface areas of soil particles." *J. Geotech. Geoenviron. Eng.* 146 (2): 4019126. https://doi.org/10.1061/(ASCE)GT.1943-5606.0002198.

Martin, R. T. 1960. "Adsorbed water on clay: A review." *Clays Clay Miner.* 9 (4): 28–70. https://doi.org/10.1346/CCMN.1960.0090104.

Mitchell, J. K., and K. Soga. 2005. *Fundamentals of soil behavior*. New York: Wiley.

Mooney, R. W., A. G. Keenan, and L. A. Wood. 1952. "Adsorption of water vapor by montmorillonite. II. Effect of exchangeable ions and lattice swelling as measured by X-ray diffraction." *J. Am. Chem. Soc.* 74 (6): 1371–1374. https://doi.org/10.1021/ja01126a002.

Richards, S., and A. Bouazza. 2007. "Determination of particle density using water and gas pycnometry." *Géotechnique* 57 (4): 403–406. https://doi.org/10.1680/geot.2007.57.4.403.

Villar, M. V., and A. Lloret. 2004. "Influence of temperature on the hydro-mechanical behaviour of a compacted bentonite." *Appl. Clay Sci.* 26 (1): 337–350. https://doi.org/10.1016/j.clay.2003.12.026.

Zhang, C., and N. Lu. 2018a. "Measuring soil-water density by helium pycnometer." *J. Geotech. Geoenviron. Eng.* 144 (9): 02818002. https://doi.org/10.1061/(ASCE)GT.1943-5606.0001929.

Zhang, C., and N. Lu. 2018b. "What is the range of soil water density? Critical reviews with a unified model." *Rev. Geophys.* 56 (3): 532–562. https://doi.org/10.1029/2018RG000597.

Zhang, C., and N. Lu. 2020. "Soil sorptive potential: Its determination and predicting soil water density." *J. Geotech. Geoenviron. Eng.* 146 (1): 4019118. https://doi.org/10.1061/(ASCE)GT.1943-5606.0002188.

Zhou, B., and N. Lu. 2021. "Assessments of water sorption methods to determine soil's specific surface area." *J. Geotech. Geoenviron. Eng.* 147 (8): 4021066. https://doi.org/10.1061/(ASCE)GT.1943-5606.0002579.

Downloaded from ascelibrary.org by University of Wisconsin-Madison on 05/24/23. Copyright ASCE. For personal use only; all rights reserved.